Article

Novel learning for control of nonlinear spacecraft dynamics

Bo-Ruei Huang [1] and Timothy Sands [2,*]

[1] Sibley School of Mechanical and Aerospace Engineering, Cornell University, Ithaca, NY 14853, USA; bh574@cornell.edu
[2] Department of Mechanical Engineering (CVN), Columbia University, New York, NY 10027 USA
* Correspondence: dr.timsands@caa.columbia.edu

Abstract: With correct dynamic system parameters (embodied in self-awareness statements), a controller can provide precise signals for tracking desired state trajectories. If dynamic system parameters are initially guessed incorrectly, a learning method may be used to find the correct parameters. In the deterministic artificial intelligence method, self-awareness statements are formed as mathematical expressions of the governing physics. When the nonlinear, coupled expressions are precisely parameterized as the product of known matrix components and unknown victrix (i.e., a regression form) tracking errors may be projected onto the known matrix to update the unknown victrix in an optimal form (in a two-norm sense). In this work, a modified learning method is proposed and proved to have global convergence of both state error and parameter estimation error. The modified learning method is compared with those in the prequels using simulation experiments of three-dimensional rigid body dynamic rotation motion. The modified approach is two magnitudes better than the methods in the prequels in terms of state error convergence.

Keywords: nonlinear systems; mechanics; spacecraft attitude control; deterministic artificial intelligence; regression, learning

1. Introduction

Consider intricate robotic operations in low-earth orbit near the space station as displayed in figure 1, where considerable human intervention is available. Next contemplate the requirements to autonomously do such operations in far distant cis-lunar orbits. The latter systems must be able to learn in real-time dynamic changes that occur when the space robot grasps and grapples targeted spacecraft. Dynamics and control issues associated with rendezvous in Cis-lunar space near rectilinear halo orbits were investigated in [1] where a fully-safe, automatic rendezvous strategy was developed between a passive vehicle and an active one orbiting around the Earth–Moon L2 Lagrangian point.

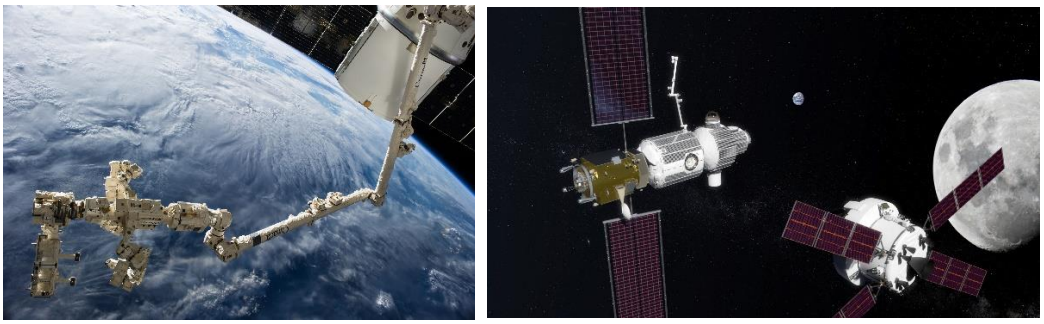

(**a**) (**b**)

Figure 1. (**a**) The International Space Station's Canadarm2 and Dextre carry the Rapidscat instrument assembly after removing it from the trunk of the SpaceX Dragon cargo ship (upper right),

 doi:10.20944/preprints202301.0472.v1

which is docked to the nadir port of the Harmony node. (**b**) NASA Gateway would support a growing space economy Photos taken from [2] and [3] respectively in compliance with NASA's image use policy [4].

Bando, et. al, [5] proposed a chattering attenuation sliding mode control utilizing the eigen structure of the linearized flow around a libration point of the Earth-Moon circular restricted three-body problem, and this novel article serves as a reminder of the prevalence of linearization when dealing with multiple, coupled nonlinear equations. In 2021, Colombia presented a guidance, navigation and control framework for 6 degrees of freedom (6DOF) coupled Cislunar rendezvous and docking, and the article highlighted the importance of dealing with full, coupled translational-rotational dynamics of multi-body (i.e., highly flexible) dynamics seeking guaranteed coupled-state estimation [6]. Immediately that same year [7], new techniques for highly flexible multi-body space robotics were proposed as a competing narrative to the just-proposed "whiplash compensation" of flexible space robotics [8]. China now has two robotic arms attached to its space station [9], where large robotic arm can "crawl" along the outside of the spacecraft [10].

Meanwhile, Zhang et. al, proposed an adaptive control strategy based on the full, nonlinear equations accounting for modeling uncertainties using an adaptive neural network amidst external disturbances [11].

In 2020, deterministic artificial intelligence was proposed by Smeresky et. al. [12], which stated that the system *dynamics constitute a feedforward* control when paired with analytic trajectories; and when the dynamics are expressed in a canonical regression form, optimal feedback (in the two-norm sense) can aid control of spacecraft attitude. The method stems from incremental development of a common nonlinear adaptive scheme offered by Slotine [13] for spacecraft attitude control, where elements of classical feedback were eliminated in 2020 foremost applied to unmanned underwater robotics [14]. The burgeoning lineage of research continued in 2022, when Sandberg et. al. [15] compared several trajectory-generation schemes and a nominal learning method based on the regression model, where applied torque is estimated by an enhanced Luenberger observer. Very shortly afterwards, Raigoza [16] augmented Sandberg's trajectory generators with autonomous collision avoidance. In November 2022, Wilt examined efficacy in the face of simulated craft damage and environmental disturbances [17].

In prequel works [12–17], the error convergence property is obtained using the proper design of the trajectory generation process. However, if the external disturbance makes the current state deviate from the trajectory, even if the system parameter is already converged to a correct value, the trajectory will need to be re-calculated to fit the current state, so that the deterministic artificial intelligence can continue to drive the system using optimal feedforward control signal.

As a result, provided the initial error between the current state and the current desired trajectory as well as incorrect initial parameter value, the goal of the modified learning approach proposed in this manuscript is to guarantee the convergence to zero of both parameter error and the state error. This work focuses on the rotation rate control problem of a spacecraft and provided 2 ways of modification to the learning phase of the deterministic artificial intelligence *algorithm and* compared them with the original deterministic artificial intelligence using simulation in MATLAB®. Moreover, the modified method can be proved to make the error converge to zero using similar way as how Slotine and Li [13] proved the stability of the non-linear system controlled by some specific feed-forward/feed-back controllers. That is, the Lyapunov candidate function is provided, and the time derivative of the candidate function can be proved to be negative with the proposed modified learning method.

Main contribution of the study. *A novel, stable learning approach is proposed to enhance deterministic artificial intelligence and efficacy amidst external disturbances is evaluated.*

2. Materials and Methods

Preprints (www.preprints.org) | NOT PEER-REVIEWED | Posted: 26 January 2023 doi:10.20944/preprints202301.0472.v1

2.1. Spacecraft Rotation Rate Control

The spacecraft rotation rate control problem focuses on applying torque so that the rotation rate of a spacecraft converges to the desired value. The dynamic can be described by the Euler equation (displayed in equation (1)). Euler's moment equations can be parameterized in canonical regression form. This full form of the coupled, nonlinear equations whose importance was highlighted by the research cited in the Introduction.

$$\tau = I\dot{\omega} + \omega \times I\omega = \underbrace{\begin{bmatrix} \dot{\omega}_x & \dot{\omega}_y - \omega_x\omega_z & \dot{\omega}_z + \omega_x\omega_y & -\omega_y\omega_z & \omega_y^2 - \omega_z^2 & \omega_y\omega_z \\ \omega_x\omega_z & \dot{\omega}_x + \omega_y\omega_z & \omega_z^2 - \omega_x^2 & \dot{\omega}_y & \dot{\omega}_z - \omega_x\omega_y & -\omega_x\omega_z \\ -\omega_x\omega_y & \omega_x^2 - \omega_y^2 & \dot{\omega}_x - \omega_y\omega_z & \omega_x\omega_y & \dot{\omega}_y + \omega_x\omega_z & \dot{\omega}_z \end{bmatrix}}_{\Phi} \underbrace{\begin{Bmatrix} I_{xx} \\ I_{xy} \\ I_{xz} \\ I_{yy} \\ I_{yz} \\ I_{zz} \end{Bmatrix}}_{\Theta} \quad (1)$$

The matrix Φ is the matrix of known, which is composed of the current state and the rate of the state (ω and $d\omega/dt$). The matrix Θ is the vector of the unknown, which is composed of system parameters, in this case, the moment of inertia. The way of formulation shows that it is possible to estimate the moment of inertia with the correct measurement of the current state.

2.2. Original deterministic artificial intelligence control

The idea of deterministic artificial intelligence is that if the matrix of the unknown can be estimated and the desired trajectory of the state is given, the optimal control signal will be multiplying the desired matrix of known (Φ_d), which includes the information of the current desired state, with the best guess of the parameter ($\hat{\theta}$). This turns the system dynamic to equation (2).

$$\tau = \Phi\Theta \rightarrow u \equiv \Phi_d\hat{\theta} \quad (2)$$

However, the $\hat{\Theta}$ can be incorrect or changed in the middle of operation. Therefore, a learning approach should be provided so that the vector of the unknown can converge to a correct value. The original learning approach in the space rotation rate control problem is described in equation 3.

$$\dot{\hat{\theta}} = \Phi^H\left(\tau_{applied} - \Phi\hat{\theta}\right) \quad (3)$$

Where $\tau_{applied}$ is the controller torque output, and the capital H means the pseudo inverse of a non-square matrix. In short, this provided a way to turn the difference between the applied torque and the expected torque into the parameter error, which should be a minimal square error estimation using the information in the current time stamp. Concerning the stability of the parameter estimation, the learning of the parameter is applied incrementally.

Additionally, deterministic artificial intelligence requires a trajectory generation process to produce a trajectory that leads from the current state to the desired state. If the current state deviates undesirably from the trajectory, it is better to update the trajectory, or the error of the state may accumulate. Please be aware that the desired state of the trajectory generation is not the desired state of the controller, which follows the output of the trajectory generator by making the trajectory the desired state of the controller should follow. In this manuscript, all the "desired states" mentioned are the desired state for the controller, if not specifically noted.

2.3. Modified Learning Method, a General Version

The target of the modification is that if the learning approach can also guarantee to decrease the error in the current state when doing the parameter estimation, the chance of regenerating trajectory can be decreased because the error is kept from growing, which increases the robustness. In a general version of the modification, we consider all the

Preprints (www.preprints.org) | NOT PEER-REVIEWED | Posted: 26 January 2023 doi:10.20944/preprints202301.0472.v1

systems that can be expressed in the regression form, as in equation (2), where the information of the current state is provided in the matrix of known. To study the error of the parameters and state, the error between the desired matrix of known and the current matrix of known is noted as ϕ, and the error of the unknown vector is noted as θ. Equation (2) can therefore be turned into equation (4). In this case, the goal becomes driving both ϕ and θ to 0 simultaneously using a modified learning method.

$$\Phi\theta + \phi\hat{\Theta} = 0 \; where \; \phi = \Phi_d - \Phi \; and \; \theta = \Theta - \hat{\Theta} \tag{4}$$

Considering the Lyapunov candidate function described in equation (5), the function value must decrease to 0 if both ϕ and θ goes to 0. If there is a parameter update approach $\dot{\theta}$ that makes the candidate function globally stable, it is very likely that the error of the state ϕ goes to 0 together with θ. Equation(7) shows that if $\dot{\theta}$ is taken in a form of equation(6), and considering equation (4) and the time derivative of equation (4), the time derivative of the Lyapunov function will be globally negative, and leads to the global stability of the system as long as the matrix G is positive definitive.

$$V = \hat{\Theta}^T\phi^T\phi\hat{\Theta} + \theta^T\theta \tag{5}$$

$$\dot{\theta}^T = \hat{\Theta}^T\phi^T((\Phi\dot{\Phi}^H)(\Phi^H + \Phi^T)^H + (\Phi^H + \Phi^T)^T G(\Phi^H + \Phi^T)) \tag{6}$$

$$\frac{\dot{V}}{2} = \left[\hat{\Theta}^T\phi^T\Phi\dot{\Phi}^H - \dot{\theta}^T\Phi^H - \dot{\theta}^T\Phi^T\right]\phi\hat{\Theta} = \hat{\Theta}^T\phi^T(\Phi^H + \Phi^T)^T G(\Phi^H + \Phi^T)\phi\hat{\Theta} \tag{7}$$

The modified learning method provided here guarantees that the Lyapunov function always goes to zero. However, if the rank of the matrix of known is not as much as the number of the unknown parameter, it is possible that the state won't converge when the Lyapunov function goes to zero. In the target application in this manuscript, the rank of the matrix of known is 3 while the parameter number in the vector of unknown is 6, this makes the learning method provided unable to guarantee convergence. One example is that when the unknown parameter happens to be correct while the state error exists, the state error will not be going to be zero. This can be seen in equation (2) that when $\widehat{\Theta} = \Theta$, the term $\widehat{\Theta}^T\phi^T = \widehat{\Theta}^T(\Phi_d - \Phi)^T$ will always be 0. When Φ has smaller rank than the number of unknowns, it is possible that $\widehat{\Theta}^T\phi^T$=0 when ϕ is not zero.

Another concern of using this method is that the calculation of $\dot{\Phi}$ is prone to noises and will cause latency in the real-time calculation because it requires the knowledge of the double derivative of the rotation rate, which generally requires special treatments like the smoothing process.

2.4. Modified Learning Method, a Specific Version

To avoid the problem mentioned in 2.3, mainly the rank issue of the known matrix, a specific version of the modified learning method is provided for the rotation rate controller. The non-regression form of the system dynamic is considered in equation (8), and the modified learning method is provided in equation (10) which utilizes both the state error as well as parameter error. Also, the character "i" means the error in the inertia matrix in a 3*3 form rather than in a 1*6 unknown vector. The torque input to the system is slight modified from $\omega_d \times I\omega_d$ to $\omega_d \times I\omega$, which improves the global stability but won't affect the feed forward optimality in the deterministic artificial intelligence much when the state is very close to the desired value.

$$I\dot{\omega} + \omega \times I\omega = \hat{I}\dot{\omega}_d + \omega_d \times I\omega \; where \; \hat{\imath} = \hat{I} - I \; and \; \omega' = \omega - \omega_d \tag{8}$$

$$I\dot{\omega}' = -(\omega' \times I\omega_d + \omega' \times I\omega') + \left(i'^{\dot{\omega}_d} + \omega_d \times i\omega_d + \omega_d \times i\omega'\right) = C\omega' + K\theta \tag{9}$$

$$\dot{\theta} = -Q\omega' - R\theta \tag{10}$$

Preprints (www.preprints.org) | NOT PEER-REVIEWED | Posted: 26 January 2023 doi:10.20944/preprints202301.0472.v1

The equation (8) is rearranged to equation (9), and the θ, again, means the inertia in a unknown vector form. To proof the global convergence of both state error ω' and parameter error θ, another Lyaponuv function (equation (11)) is provided, which have a physical meaning close to the square error of the whole system, where the state square error is weighted by the inertia. If the Q term in equation (10) is the transpose of K term in equation (9), and the R term in equation (10) is positive definite, the Lyapunov function will be stable globally, as shown in equation (12), and can achieve zero state error and parameter error is guaranteed. Finally, the parameter vector is chosen based on equation (13), derived from equation (4), and the value is used for modified learning method in equation (10).

$$V = \omega'^T I\omega' + \theta^T\theta \tag{11}$$

$$\begin{aligned}\frac{\dot{V}}{2} &= \omega'^T I\dot{\omega}' + \theta^T\dot{\theta} = \omega'^T[-(\omega' \times I\omega_d + \omega' \times I\omega')]\dot{\omega}' + \theta^T(K^T - Q)\omega' - \theta^T R\theta \\ &= \theta^T(K^T - Q)\omega' - \theta^T R\theta = -\theta^T R\theta < 0\end{aligned} \tag{12}$$

$$\theta = -\Phi^H\phi\hat{\theta} \tag{13}$$

2.5. Simulation

The trajectory tracking of the rotation rate controller will be simulated. In the simulation, the trajectory is generated using arbitrary test torque, as shown in equation (14). The controller does not possess the test torque value, but instead receives a stream of desired rotation rate and the time derivative of the rotation rate. The idea is that if the deterministic artificial intelligence can track the test trajectory, it should also be able to track any trajectory generated by another trajectory planner.

$$I\dot{\omega}_d + \omega_d \times I\omega_d = \tau_{test} \tag{14}$$

Two types of performance matrices are considered: norm ratio of the state error, and the norm ratio of the parameter error, in equation (16). The result is plotted in Section 3.

$$\begin{aligned}State\ error\ norm\ ratio &= ln\left(\frac{||\omega'||_2^2}{||\omega_d||_2^2}\right) \\ Parameter\ error\ norm\ ratio &= \frac{||\theta'||_2^2}{||\theta||_2^2}\end{aligned} \tag{15}$$

3. Results

In this section, simulation results of the rotation rate problem (section 2.1) under different condition is presented, and the performance of both types of modification (general version in section 2.3 and specific version in 2.4) is compared with the original deterministic artificial intelligence (section 2.2) learning approach.

3.1. Performance Comparison without the Product of Inertia

This case aims at testing the learning method when there is no product of inertia value in both the system's true parameter and the initial estimation of the unknown vector. The initial condition and the system parameters are listed in Table 1. The norm ratio of the state error and parameter error is shown in Fig. 1. Also, the G in equation (7) and the R in equation (10) will be a scaler "r" multiplied by a 6*6 identity matrix, and this form of G and R will be used in all the cases presented in this manuscript.

Table 1. Initial condition for the simulation in section 3.1.

Variable	Value	Variable	Value	Variable	Value

Preprints (www.preprints.org) | NOT PEER-REVIEWED | Posted: 26 January 2023 doi:10.20944/preprints202301.0472.v1

I_{xx}	1	I_{yy}	2	I_{zz}	3
I_{xy}	0.2	I_{xz}	0.3	I_{yz}	0.4
$\omega_{init,x}$	0.02	$\omega_{init,y}$	0.03	$\omega_{init,z}$	0.01
$\tau_{test,x}$	5	$\tau_{test,y}$	2	$\tau_{test,z}$	-2
r	3				

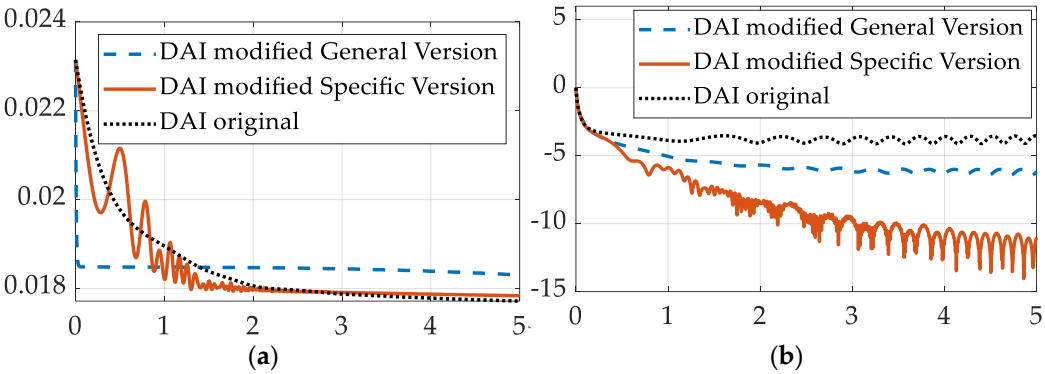

Figure 1. The convergence of the parameter error and state error. (**a**) Parameter error norm ratio on the ordinant versus time in seconds on the abscissa. (**b**) State error norm ratio on the ordinant versus time in seconds on the abscissa.

Table 2. Convergence of inertia estimation and tracking errors

Figure of merit	Original method (prequels)	Proposed version general	Proposed version specific
Parameter error mean	0.0019	0.0027	0.0029
Parameter error deviation	0.0032	0.0037	0.0064
Mean tracking error	0.0401	-0.0094	-0.00037
Tracking error deviation	0.1518	0.0138	0.0065

3.2. Performance Comparison with the Product of Inertia

This case is similar to section 3.1, but the product of inertia values in both the system's true parameter and the initial estimation of the unknown vector is not zero. The initial condition and the system parameters are listed in Table 3. The norm ratio of the state error and parameter error is shown in Fig. 2.

Table 3. Initial condition for the simulation in section 3.2.

Variable	Value	Variable	Value	Variable	Value
I_{xx}	1	I_{yy}	2	I_{zz}	1
I_{xy}	0.2	I_{xz}	0.3	I_{yz}	0.4
$\hat{I}_{xx,init}$	1.06	$\hat{I}_{yy,init}$	1.90	$\hat{I}_{zz,init}$	1.15
$\hat{I}_{xy,init}$	0.21	$\hat{I}_{xz,init}$	0.31	$\hat{I}_{yz,init}$	0.41
$\omega_{init,x}$	0.02	$\omega_{init,y}$	0.03	$\omega_{init,z}$	0.01
$\tau_{test,x}$	5	$\tau_{test,y}$	2	$\tau_{test,z}$	-2
r	3				

Preprints (www.preprints.org) | NOT PEER-REVIEWED | Posted: 26 January 2023 doi:10.20944/preprints202301.0472.v1

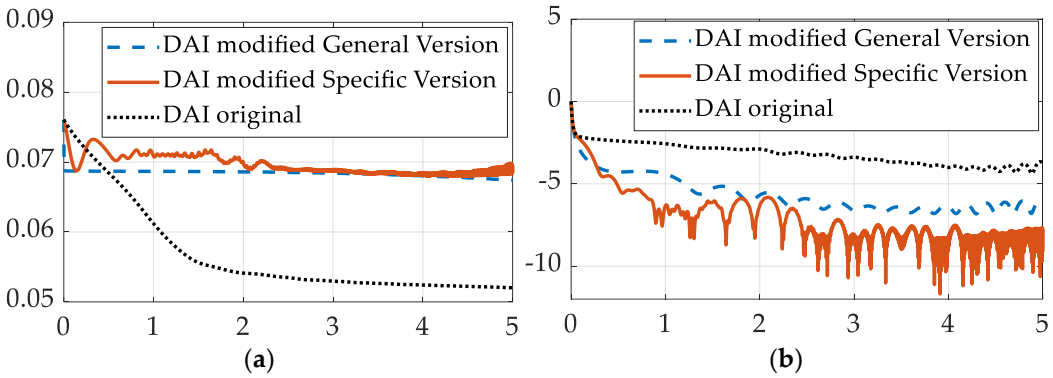

Figure 2. The convergence of the parameter error and state error. (**a**) Parameter error norm ratio on the ordinant versus time in seconds on the abscissa. (**b**) State error norm ratio on the ordinant versus time in seconds on the abscissa.

3.3. Performance Comparison with Different r value

This case shows for the modified learning method (Specific Version) how the r value, which can be seen as the "magnitude" of the G in equation (7) and the R in equation (10), affects the final result. The initial condition and parameters used in this case are identical to case 3.2 and can be checked in Table 3, except for the r value.

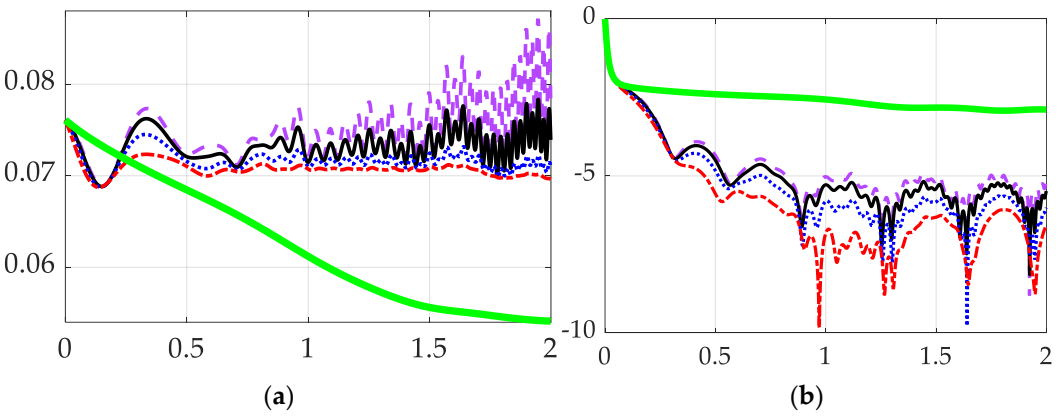

Figure 3. The convergence of the parameter error and state error. Original deterministic artificial intelligence displayed by a thick, solid green line, dashed purple line displays $r = 0.5$, thin solid black line displays $r = 1$, dotted blue line displays $r = 2$, dot-dashed red line displays $r = 4$, (**a**) Parameter error norm ratio on the ordinant versus time in seconds on the abscissa. (**b**) State error norm ratio on the ordinant versus time in seconds on the abscissa.

Table 4. Convergence of inertia estimation and tracking errors

Figure of merit	Original method (prequels)	Modified with $r = 0.5$	Modified with $r = 1$	Modified with $r = 2$	Modified with $r = 4$
Parameter error mean	0.0247	0.0351	0.0348	0.0345	0.0341
Parameter error deviation	0.0124	0.0306	0.0272	0.0239	0.0217
Mean tracking error	-0.0401	-0.0033	-0.0033	-0.0033	-0.0034
Tracking error deviation	0.1761	0.0296	0.0246	0.0189	0.0143

4. Discussion

In sections 3.1 and 3.2, the modified learning method yields better state error convergence than the original method. For the specific version of the modified method, the final state error norm ratio is about 2 magnitudes smaller (rough order $\times 10^{-8}$ compared with $\times 10^{-3}$) than the original learning method, due to the data are shown in both Fig. 1 and 2.

In section 3.1, all the learning methods yield similar convergence rate of the parameter error when the moment of inertia matrix doesn't contain the product of inertia terms,

Preprints (www.preprints.org) | NOT PEER-REVIEWED | Posted: 26 January 2023 doi:10.20944/preprints202301.0472.v1

as shown in the left part of Fig. 1. However, when the moment of inertia matric contains nonzero product of inertia, as has been done in section 3.2, the left part of Fig.2 shows that the modified methods are not better than the original method.

Table 5. Percent performance enhancement: Convergence of inertia estimation and tracking errors

Figure of merit	Original method (prequels)	Proposed version general	Proposed version specific
Parameter error mean	**0%**	42%	53%
Parameter error deviation	**0%**	16%	100%
Mean tracking error	0%	–77%	**–99%**
Tracking error deviation	0%	–91%	**–96%**

In section 3.3, Fig. 3 shows that when the magnitude of R in equation (10) goes bigger, the convergence rate also increases. Because equation (12) states that the convergence rate of the Lyapunov function (equation (11)) is only determined by the size of R and θ, the result in section 3.3 is reasonable.

Table 6. Percent performance enhancement: Convergence of inertia estimation and tracking errors

Figure of merit	Original method (prequels)	Modified with $r = 0.5$	Modified with $r = 1$	Modified with $r = 2$	Modified with $r = 4$
Parameter error mean	0.00%	-42.11%	-40.89%	-39.68%	-38.06%
Parameter error deviation	0.00%	-146.77%	-119.35%	-92.74%	-75.00%
Mean tracking error	0.00%	91.77%	91.77%	91.77%	91.52%
Tracking error deviation	0.00%	83.19%	86.03%	89.27%	91.88%

From the convergence condition of errors in Fig. 1, 2, and 3, it can be concluded that the convergence trajectories of the specific version of the modified learning method are more "bumpy" and contains more jitters and oscillations. This phenomenon may result from the way of θ value determination provided in equation (13), which only consider the data in the current time stamp, and the indeterminate nature of equation (13) makes the estimation of θ very unstable.

It can be concluded that the specific version of the modified learning method can achieve the convergence of both parameter error and state error in the simulation done in this manuscript, which can increase the robustness of the rotation rate controller.

4.1. Recommended Future Work

From the parameter error data of the specific version of modified method in Fig. 1~3, the increasing jitters can be observed. The reason for such instability after the convergence is unclear. It could result from the numerical instability of the chosen ODE solver and the options given to it, or the indeterminate way used for determining θ value in equation (13).

Moreover, the property of the "general version of modified learning method" hasn't been explored carefully because it is not suitable in this case by nature. Also, a better way of estimating θ may improve the result of the modified learning method as well. Finally, a better way of choosing the G in equation (7) and the R in equation (10) is also an interesting topic.

Conflicts of Interest: The authors declare no conflict of interest.

Appendix A

The MATLAB® code used in this manuscript is pasted below. The program utilizes the ode45 solver to simulate the response of the overall system combining the controller and the controlled system.

Preprints (www.preprints.org) | NOT PEER-REVIEWED | Posted: 26 January 2023 doi:10.20944/preprints202301.0472.v1

```
%% deterministic artificial intelligence 3D Euler Test
clc; clear; close all
% syms
syms fwx(t) fwy(t) fwz(t)
syms Ixx Ixy Ixz Iyy Iyz Izz real
syms wx wy wz dwx dwy dwz ddwx ddwy ddwz real
w = [fwx;fwy;fwz];
wT = [fwx fwy fwz];
dw = diff(w,t);
ddw = diff(dw,t);
I = [Ixx Ixy Ixz; Ixy Iyy Iyz; Ixz Iyz Izz];
PhTh = I*dw + cross(w,I*w);
Peq = PhTh == 0;
[P, sbz] = equationsToMatrix(Peq, [Ixx Ixy Ixz Iyy Iyz Izz]);
dP = diff(P,t);
sP = subs(P, [fwx fwy fwz diff(wT,t) diff(diff(wT,t),t)], [wx wy wz dwx dwy dwz ddwx ddwy ddwz]);
sdP = subs(dP, [fwx fwy fwz diff(wT,t) diff(diff(wT,t),t)], [wx wy wz dwx dwy dwz ddwx ddwy ddwz]);
sfP = symfun(sP, [wx wy wz dwx dwy dwz ddwx ddwy ddwz]);
sfdP = symfun(sdP, [wx wy wz dwx dwy dwz ddwx ddwy ddwz]);

%%
syms wdx wdy wdz dwdx dwdy dwdz real
syms ixx ixy ixz iyy iyz izz real
w = [wx;wy;wz];
wd = [wdx;wdy;wdz];
dwd = [dwdx dwdy dwdz]';
i = [ixx ixy ixz; ixy iyy iyz; ixz iyz izz];
Ki = i'*dwd + cross(wd,i*wd) + cross(wd,i*w);
Keq = Ki == [0;0;0];
[K, sbz] = equationsToMatrix(Keq, [ixx ixy ixz iyy iyz izz]);
fK = symfun(K, [wx wy wz wdx wdy wdz dwdx dwdy dwdz]);

%% param
clc; close all
% p.J = [1 0 0; 0 2 0; 0 0 3];
p.J = [1 0.2 0.3; 0.2 2 0.4; 0.3 0.4 1];
p.dwd = [1 1 1]';
p.P = MATLAB®Function(sfP);
p.dP = MATLAB®Function(sfdP);
p.K = MATLAB®Function(fK);
p.G = 3*eye(6);
Jt = [p.J(1,1);p.J(1,2);p.J(1,3);p.J(2,2);p.J(2,3);p.J(3,3)];
% time
tfinal = 5;
deltat = 0.001;
t = 0:deltat:tfinal;% for evaluating solution
% solve the ODE
z0 = [1 0 0 0 0 0 0 0.08 0.08 0.04 1.06 0.21 0.31 1.90 0.41 1.15]';
options = odeset('absTol',1e-10,'relTol',1e-10);
% The simulation for the general version of modified learning method
[t_dai, z_dai] = ode45(@(t,z)deterministic_artificial_intelligence_modified_general(t,z,p), t, z0, options);
% The simulation for the specific version of modified learning method
[t_dmd, z_dmd] = ode45(@(t,z)deterministi_artificia_intelligence_modified_specific(t,z,p), t, z0, options);
% The simulation for the original version of learning method
[t_dor, z_dor] = ode45(@(t,z)deterministic_artificial_intelligence_original(t,z,p), t, [z0;0;0;0], options);
%% Plot parameter estimations and state trajectories
figure()
plot(t_dai, z_dai(:,11),t_dai, z_dai(:,14),t_dai, z_dai(:,16))
figure()
plot(t_dmd, z_dmd(:,11),t_dmd, z_dmd(:,14),t_dmd, z_dmd(:,16))
figure()
plot(t_dor, z_dor(:,11),t_dor, z_dor(:,14),t_dor, z_dor(:,16))
figure()
plot(t_dai, z_dai(:,7),t_dor, z_dor(:,7),t_dmd, z_dmd(:,7),t_dai, z_dai(:,10))
```

Preprints (www.preprints.org) | NOT PEER-REVIEWED | Posted: 26 January 2023 doi:10.20944/preprints202301.0472.v1

```
legend('Modified 1', 'Original', 'Modified 2', 'Desired');
figure()
plot(t_dai, z_dai(:,6),t_dor, z_dor(:,6),t_dmd, z_dmd(:,6),t_dai, z_dai(:,9))
legend('Modified 1', 'Original', 'Modified 2', 'Desired');
figure()
plot(t_dai, z_dai(:,5),t_dor, z_dor(:,5),t_dmd, z_dmd(:,5),t_dai, z_dai(:,8))
legend('Modified 1', 'Original', 'Modified 2', 'Desired');

%% Analysis the norm rates
% inertia norm
J_dai = z_dai(:,11:16);
J_dmd = z_dmd(:,11:16);
J_dor = z_dor(:,11:16);
n = length(t_dai);
nJ_dai = vecnorm(J_dai'-Jt*ones(1,n))/norm(Jt);
nJ_dmd = vecnorm(J_dmd'-Jt*ones(1,n))/norm(Jt);
nJ_dor = vecnorm(J_dor'-Jt*ones(1,n))/norm(Jt);
figure()
plot(t_dai, nJ_dai, t_dmd, nJ_dmd, t_dor, nJ_dor);
legend('deterministic artificial intelligence modified General Version', 'deterministic artificial intelligence
modified Specific Version', 'deterministic artificial intelligence original');
title('Convergence of the parameter error norm ratio');
xlabel('time (s)');
ylabel('Parameter error norm ratio');
% state error norm
dw_dai = z_dai(:,5:7)-z_dai(:,8:10);
nw_dai = vecnorm(dw_dai')./vecnorm(z_dai(:,8:10)');
dw_dmd = z_dmd(:,5:7)-z_dmd(:,8:10);
nw_dmd = vecnorm(dw_dmd')./vecnorm(z_dmd(:,8:10)');
dw_dor = z_dor(:,5:7)-z_dor(:,8:10);
nw_dor = vecnorm(dw_dor')./vecnorm(z_dor(:,8:10)');
figure()
plot(t_dai, log(nw_dai), t_dmd, log(nw_dmd), t_dor, log(nw_dor));
legend('deterministic artificial intelligence modified General Version', 'deterministic artificial intelligence
modified Specific Version', 'deterministic artificial intelligence original');
title('Convergence of the state error norm ratio');
xlabel('time (s)');
ylabel('State error norm ratio');

%% Function
function zdot = deterministic_artificial_intelligence_modified_general(t, z, p)
    q = z(1:4);
    w = z(5:7);
    wd = z(8:10);
    th = z(11:16); % theta hat
    Jh = [th(1) th(2) th(3); th(2) th(4) th(5); th(3) th(5) th(6)];
    % generate trajectory
    [sdwd,sddwd] = traj_gen(t,wd,p);
    % generate feed forward control torque
    tau = Jh*sdwd + cross(wd', Jh*wd)';
    % update the dynamic of the system
    dw = p.J\(tau-cross(w', p.J*w)');
    dq = 0.5*quatmultiply([0 w'],q');
    % update the parameter estimation
    ddw = [0;0;0];
    Pd = p.P(wd(1),wd(2),wd(3),sdwd(1),sdwd(2),sdwd(3),sddwd(1),sddwd(2),sddwd(3));
    P = p.P(w(1),w(2),w(3),dw(1),dw(2),dw(3),0,0,0);
    dP = p.dP(w(1),w(2),w(3),dw(1),dw(2),dw(3),ddw(1),ddw(2),ddw(3));
    ph = Pd-P; %P - Pd;
    A = dP*pinv(P)*pinv(P' + pinv(P));
    B = (P' + pinv(P))'*p.G;
    dth = (th'*ph'*(A+B))';
    if abs(t-round(t)) < 0.001
        disp(t)
    end
```

Preprints (www.preprints.org) | NOT PEER-REVIEWED | Posted: 26 January 2023 doi:10.20944/preprints202301.0472.v1

```
    zdot = [dq';dw;sdwd;dth];
end

function zdot = deterministic_artificial_intelligence_modified_specific(t, z, p)
    q = z(1:4);
    w = z(5:7);
    wd = z(8:10);
    th = z(11:16); % theta hat
    Jh = [th(1) th(2) th(3); th(2) th(4) th(5); th(3) th(5) th(6)];
    % generate trajectory
    [sdwd,sddwd] = traj_gen(t,wd,p);
    % generate feed forward control torque
    tau = Jh*sdwd + cross(wd', Jh*wd)';
    % update the dynamic of the system
    dw = p.J\(tau-cross(w', p.J*w)');
    dq = 0.5*quatmultiply([0 w'],q');
    % update the parameter estimation
    Pd = p.P(wd(1),wd(2),wd(3),sdwd(1),sdwd(2),sdwd(3),sddwd(1),sddwd(2),sddwd(3));
    P = p.P(w(1),w(2),w(3),dw(1),dw(2),dw(3),0,0,0);
    ph = Pd-P;
    K = p.K(w(1),w(2),w(3),wd(1),wd(2),wd(3),sdwd(1),sdwd(2),sdwd(3));
    dth = -K'*(w-wd) + p.G*(pinv(P)*ph*th);
    if abs(t-round(t)) < 0.001
        disp(t)
    end
    zdot = [dq';dw;sdwd;dth];
end

function zdot = deterministic_artificial_intelligence_original(t, z, p)
    q = z(1:4);
    w = z(5:7);
    wd = z(8:10);
    th = z(11:16); % theta hat
    Jh = [th(1) th(2) th(3); th(2) th(4) th(5); th(3) th(5) th(6)];
    ei = z(17:19);
    % generate trajectory
    [sdwd,sddwd] = traj_gen(t,wd,p);
    % generate feed forward control torque
    tau = Jh*sdwd + cross(wd', Jh*wd)';
    % update the dynamic of the system
    dw = p.J\(tau-cross(w', p.J*w)');
    dq = 0.5*quatmultiply([0 w'],q');
    % update the parameter estimation
    P = p.P(w(1),w(2),w(3),dw(1),dw(2),dw(3),0,0,0);
    dth = 1.5*pinv(P)*(tau-P*th);
    e = -wd+w;
    dei = e;
    zdot = [dq';dw;sdwd;dth;dei];
end

function [dwd,ddwd] = traj_gen(t,wd,p)
    tau = [5;2;-2];
    if t>7
        tau = [0;0;0];
    end
    dwd = p.J\(tau-cross(wd', p.J*wd)');
    ddwd = [0;0;0];
end
```

References

1. Bucchioni, G.; Innocenti, M. Rendezvous in Cis-Lunar Space near Rectilinear Halo Orbit: Dynamics and Control Issues. *Aerospace* **2021**, *8*, 68.
2. Johnson, M. Space Station Robotic Arms Have a Long Reach. Available online: https://www.nasa.gov/mission_pages/station/research/news/b4h-3rd/hh-robotic-arms-reach (accessed on 23 December 2022).

3. Mahoney, E. NASA Seeks Ideas for Commercial Uses of Gateway. Available online: https://www.nasa.gov/feature/nasa-seeks-ideas-for-commercial-uses-of-gateway (accessed on 23 December 2022).
4. NASA Image Use Policy. Available online: https://gpm.nasa.gov/image-use-policy (accessed on 23 December 2022).
5. Bando, M.; Namati, H.; Akiyama, Y.; Hokamoto, S. Formation flying along libration point orbits using chattering attenuation sliding mode control. *Front. Space Technol.* **2022**, 3, 919932.
6. Colombia, F.; Colagrossi, A.; Lavagna, M. Characterization of 6DOF natural and controlled relative dynamics in cislunar space. *Acta Astronautica* **2022**, *196*, 369-379.
7. Sands, T. Flattening the Curve of Flexible Space Robotics. *Appl. Sci.* **2022**, *12*, 2992.
8. Sands, T. Optimization Provenance of Whiplash Compensation for Flexible Space Robotics. *Aerospace* **2019**, *6*(9), 93.
9. Jones, A. Chinese space station robot arm tests bring amazing views from orbit. Available online: https://www.space.com/china-space-station-wentian-robot-arm-test (accessed on 23 December 2022).
10. Jones, A. See a large robotic arm 'crawl' across China's space station. https://www.space.com/china-space-station-robot-arm-video (accessed on 23 December 2022).
11. Zhang, K.; Pan, B. Control design of spacecraft autonomous rendezvous using nonlinear models with uncertainty. *J. ZheJiang Univ.* **2022**, *56*(4), 833-842.
12. Smeresky, B.; Rizzo, A.; Sands, T. Optimal Learning and Self-Awareness Versus PDI. *Algorithms* **2020**, *13,23*.
13. Slotine, J.; Li, W. *Applied Nonlinear Control*; Prentice-Hall, Inc.: Englewood Cliffs, NJ, U.S.A., 1991; pp. 392–436.
14. Sands, T. Development of Deterministic Artificial Intelligence for Unmanned Underwater Vehicles (UUV). *J. Mar. Sci. Eng.* **2020**, *8*, 578
15. Sandberg, A.; Sands, T. Autonomous Trajectory Generation Algorithms for Spacecraft Slew Maneuvers. *Aerospace* **2022**, *9,135*.
16. Raigoza, K.; Sands, T. Autonomous Trajectory Generation Comparison for De-Orbiting with Multiple Collision Avoidance. *Sensors* **2022**, *22*, 7066. https://doi.org/10.3390/s22187066
17. Wilt, E.; Sands, T. Microsatellite Uncertainty Control Using Deterministic Artificial Intelligence. *Sensors* **2022**, *22*, 8723.